# Dual-WGAN Ensemble Model for Alzheimer's Dataset Augmentation with Minority Class Boosting

Mohammad Samar Ansari
*Faculty of Science, Business & Enterprise*
*University of Chester*
United Kingdom
m.ansari@chester.ac.uk

Kulsum Ilyas
*Z.H. College of Engineering & Technology*
*Aligarh Muslim University*
Aligarh, India
kulsumilyas64@gmail.com

Asra Aslam
*Faculty of Medicine and Health*
*University of Leeds*
United Kingdom
a.aslam2@leeds.ac.uk

***Abstract*—Deep learning models have become very efficient and robust for several computer vision applications. However, to harness the benefits of state-of-art deep networks in the realm of disease detection and prediction, it is crucial that high-quality datasets be made available for the models to train on. This work recognizes the lack of training data (both in terms of quality and quantity of images) for using such networks for the detection of Alzheimer's Disease. To address this issue, a Wasserstein Generative Adversarial Network (WGAN) is proposed to generate synthetic images for augmentation of an existing Alzheimer brain image dataset. The proposed approach is successful in generating high-quality images for inclusion in the Alzheimer image dataset, potentially making the dataset more suitable for training high-end models. This paper presents a two-fold contribution: (i) a WGAN is first developed for augmenting the non-dominant class (i.e. Moderate Demented) of the Alzheimer image dataset to bring the sample count (for that class) at par with the other classes, and (ii) another lightweight WGAN is used to augment the entire dataset for increasing the sample counts for all classes.**

***Index Terms*—Alzheimer Disease, Data Augmentation, Deep Learning, Generative Adversarial Network (GAN), Imbalanced Datasets, Wasserstein Generative Adversarial Network (WGAN).**

## I. Introduction

Alzheimer's Disease (AD) is a progressive neurological condition that starts gradually and worsens over time. Its primary onset symptom is difficulty in recalling recent events. It is an irreversible disease, and no known medication can modify its course [1]. However, there have been promising recent medical advancements [2]. As of 2020, over the world nearly 50 million people had Alzheimer's disease, and the current estimate is around 55 million, with the number of AD patients expected to reach approximately 140 million by 2050 [3]. Consequently, significant efforts have been directed towards developing onset detection tools, particularly during pre-symptomatic phases, to mitigate or prevent disease progression [4], [5]. Recent state-of-art neuro-imaging techniques like positron emission tomography (PET) and magnetic resonance imaging (MRI) have been devised and employed to identify AD biomarkers at the molecular and structural levels [6]. Through these methods, researchers have observed declines in certain brain regions' size in individuals with AD as they transition from mildly impaired cognitive abilities to Alzheimer's disease, as compared to healthy older individuals. Utilizing these brain region alterations, automated detection tools have been developed for Alzheimer's disease, as well as for other diseases (e.g., using X-ray images to identify COVID-19 progression).

Deep learning (DL), an advanced machine learning approach, has surpassed classical machine learning in its ability to detect intricate patterns within complex high-dimensional data, especially in the realm of computer vision [7]. With the advancement of neuroimaging techniques, the development of extensive multimodal neuroimaging datasets has become possible. As a result, there has been a surge of research interest in applying DL to achieve early diagnosis and automated categorization of Alzheimer's disease [8].

Utilizing deep neural networks with bio-image datasets can be challenging due to limited availability of data [9]. Data augmentation addresses this issue by creating diverse versions of the initial data through techniques like reflection, translation, and rotation. However, these basic approaches lack the ability to generate new images that retain the original sample's underlying characteristics. For specialized tasks like disease detection in MRI images, a more robust data augmentation process is crucial. This paper presents an image augmentation DL model that aims to generate new samples while preserving the intrinsic characteristics of the original dataset.

There is another complication is this entire scenario – which is the inherent imbalance present in the number of samples (images) available for the different classes. It is natural to have a very large number of 'normal' samples in any disease dataset, while the number of samples for different variations of the disease (e.g. Mild Dementia, Moderate Dementia, Very Mild Dementia, etc.) may be significantly less for some classes. This is a severe issue with ML/DL algorithms training using such datasets. This is because such algorithms tend to favor the majority class, as it has more data points to learn from. Machine learning models use balanced metrics by default, which may result in poor model performance and incorrect classification of the minority class. To deal with this problem, one possible solution is to employ sampling technique(s) if the task is a classification one with an imbalanced dataset. Downsampling and upweighting is a useful way to handle imbalanced data. In this specific context, downsampling refers

to the practice of training on a significantly reduced subset of examples from the majority class. Conversely, upweighting involves assigning an increased weight to the downsampled class, which is equivalent to the ratio by which the downsampling is performed. There are also other techniques such as Synthetic Minority Over-sampling Technique (SMOTE) and Adaptive Synthetic Sampling that can help with imbalanced datasets. In addition to these approaches, the use of Generative Networks may also be explored for this task. This paper presents one such proposal.

Generative Adversarial Networks (GANs) are a deep learning method for generative modeling, often employing convolutional neural networks. They can generate novel data instances based on the training data, aiming to replicate the statistical properties of the training set. GAN-based data augmentation outperforms na"ıve approaches, producing higher-quality generated images. GANs can create authentic-looking images, benefiting various learning scenarios, such as semi-supervised and fully supervised learning [10], and reinforcement learning, despite their initial unsupervised learning purpose [11]. GANs use a discriminator neural network to indirectly train the generator by assessing input data realism. The discriminator continuously updates, and the generator is trained to deceive it rather than minimizing distances to specific images. This unique training process enables GANs to learn and generate data without explicit supervision[1].

*Contribution:* Given the scarcity of high-quality publicly available datasets for training deep neural networks in Alzheimer's disease (AD) detection, we introduce a data augmentation model based on Wasserstein Generative Adversarial Networks (WGAN) [**?**]. This WGAN-based model utilizes AD MRI images as input data to synthetically enhance the Alzheimer's disease dataset, with a particular focus on the Moderate Demented class. The primary objective of this research is to augment the Alzheimer's disease dataset to facilitate future studies and enable the development of more efficient, automated, and accurate prognosis systems. This paper makes a dual contribution: firstly, the development of a WGAN to augment the non-dominant class (i.e. the Moderate Demented class, which only has 64 images in the original dataset, as compared to the Mild/Very-Mild/Normal classes which have 896/2240/3200 images respectively) in the Alzheimer image dataset, aligning its sample count with other classes, and secondly, the utilization of a lightweight WGAN to augment the entire dataset, thereby increasing sample counts for all classes for ensuring better training for ML/DL models.

The paper's structure is as follows: Section II provides a concise overview of relevant research. In Section III, we elaborate on the proposed approach and methodology. Section IV presents an evaluation of the system's performance and results. Finally, Section VI concludes the paper with closing remarks.

[1]https://theaisummer.com/gan-computer-vision/#vanilla-gan-generative-adversarial-networks-2014

## II. Related Work

Various models have been implemented in the literature to generate image datasets for augmenting AD MRI images. Here is a brief overview of some existing models:

Park et al. [12] employed generative adversarial networks (GANs) to predict the molecular progression of Alzheimer's disease. They utilized GANs to analyze RNA-seq data from a 5×FAD animal AD model, which replicates significant AD characteristics, including substantial amyloid deposition in the brain. Their focus was on configuring the generator to produce specific samples and identify biologically relevant genes.

Based on their findings, the researchers proposed the use of latent space interpolation to generate transition curves for several genes exhibiting pathogenic alterations from the normal to AD states. This approach revealed numerous pathogenic processes with progressive changes, such as inflammatory systems and synapse functioning. These pathways, as shown by transition curve patterns, have previously been associated with the pathogenesis of AD.

An intriguing discovery from their study was that changes in cholesterol biosynthesis commence early in the course of Alzheimer's disease, indicating that cholesterol metabolism is affected downstream of amyloid buildup and might be among the initial impacts in AD progression.

The study presented in [13] introduces a novel three-component adversarial network-based technique for Alzheimer's disease (AD) detection, known as the Brain slice generative adversarial network for Alzheimer's disease detection (BSGAN-ADD). This method combines deep convolutional neural network (CNN) based AD diagnosis with generative adversarial network (GAN) based brain slice image enhancement.

In another study by Han et al. [14], a two-step technique for detecting Alzheimer's disease at various stages is proposed. This method utilizes a Generative Adversarial Network-based approach for multiple adjacent brain MRI slice reconstruction, employing Wasserstein loss with Gradient Penalty. Three healthy slices are used to reconstruct the subsequent three unseen healthy/AD instances. The results demonstrate consistent AD detection at an early stage with an AUC of 0.780 and considerably improved detection of AD at a late stage with an AUC of 0.917 [14].

Zhou et al. [15] conducted a study demonstrating the potential of using GAN frameworks to enhance image quality and improve AD classification performance. Their approach involved combining a 3-dimensional fully convolutional network with the GAN-generated images as inputs to predict AD enormity. They assessed image quality using complex metrics like Blind/Reference-less Image Spatial Quality Evaluator (BRISQUE), and Natural Image Quality Evaluator (NIQE). The model's validation was carried out using samples from the Australian Imaging, Biomarker, and Lifestyle Flagship Study of Aging (AD data from 107 persons) and the National Alzheimer's Coordinating Center (AD data from 565 persons) [15].

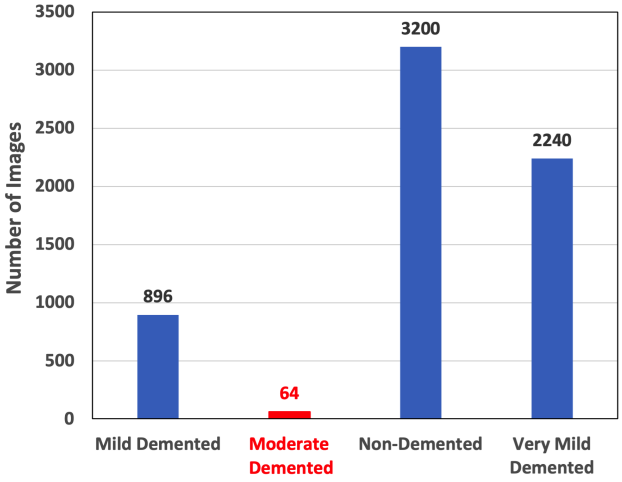


Fig. 1. Sample distribution of different classes in the chosen dataset

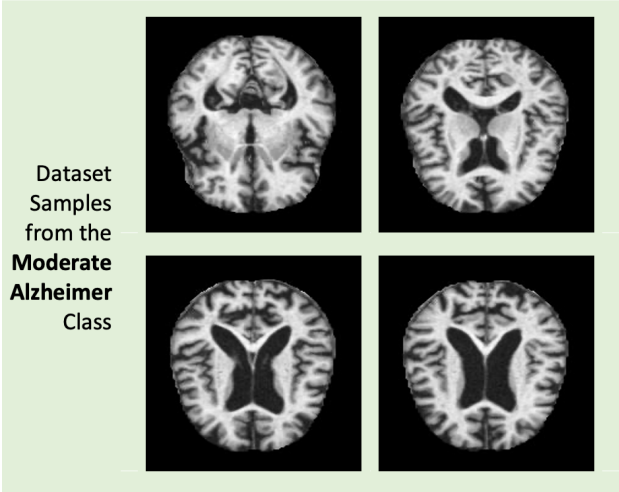


Fig. 2. Samples from the 'Moderate Demented' class of the chosen dataset

Islam and Zhang proposed a generative adversarial network-based model [16] for creating synthetic medical images, specifically targeting three stages of Alzheimer's disease: Normal Control (NC) group, Mild Cognitive Impairment (MCI) stage, and full-blown Alzheimer's Disease (AD) samples.

In their research [17], Garali et al. introduced new features derived from 1st and 2nd derivatives computed on brain PET scans to enhance picture categorization for Alzheimer's disease. The brain images were separated into volumes of interest (similar to 3D regions-of-interest) using an atlas, and the orientation field for each VOI was analyzed to assess the features' ability to distinguish AD from Healthy Control (HC). Their approach involved creating 3D gradient images, computing the first and second derivatives of each VOI, and then feeding these features into a Support Vector Machine (SVM) classifier. The classification accuracy was found to be higher when using mean, first, and second derivatives features from VOIs compared to using only the mean value.

## III. Proposed Methodology

The significance of data quality and quantity in determining the performance of deep learning models is widely acknowledged. A well-constructed dataset enables a deep learning model to learn the intrinsic data characteristics without the need for explicit programming. In this study, we propose a WGAN-based approach to synthetically generate training images. The goal is to enhance the development of deep learning models for AD detection [18].

### A. Dataset

We have adopted an open access Kaggle dataset[2], which includes only a meagre 64 MRI images in the Moderate Demented class, while including significantly higher number of images in the other categories *viz.* Mild Demented (896), Non-Demented (3200), and Very Mild Demented (2240). Fig. 1 illustrates the distribution of various classes in the chosen dataset. As alluded to briefly in Section-I, the very small number of images in the 'Moderate Demented' class creates an imbalance in the dataset (highlighted in red color), which in turn would affect model training and performance. It is therefore imperative that the number of images in the Moderate Demented class be boosted before attempting to use an augmentation approach.

The image size used for this work remains unchanged at $175 \times 175$, without any resizing, to prevent a decrease in classification accuracy due to deformations. This size selection considers the model's training duration while ensuring a high level of model efficacy. Sample images from the dataset are showcased in Fig. 2.

### B. The Model

As is now widely known, a Generative Adversarial Network (GAN) is a type of deep learning model used for generative modelling. The primary objective of a GAN is to generate new data instances that resemble a given training dataset. It essentially comprises of two distinct neural networks: the generator and the discriminator. The former is primarily responsible for producing synthetic data samples, while the latter tries to distinguish between the real data (i.e. the training data) and the fake data (i.e. the samples generated by the generator). The main goal of the critic is to estimate the Wasserstein distance (also known as Earth Mover's distance[3]) between the real data distribution and the generated data distribution. During the training process, the critic aims to provide accurate estimates of the Wasserstein distance, while the generator tries to produce data samples that minimize this distance. The aim of the GAN training process is to reach a point where the generated data is highly realistic and closely matches the characteristics of the original training data.

[2]https://www.kaggle.com/datasets/tourist55/alzheimers-dataset-4-class-of-images

[3]The Earth Mover's Distance; available at: https://homepages.inf.ed.ac.uk/rbf/CVonline/LOCAL_COPIES/RUBNER/emd.htm

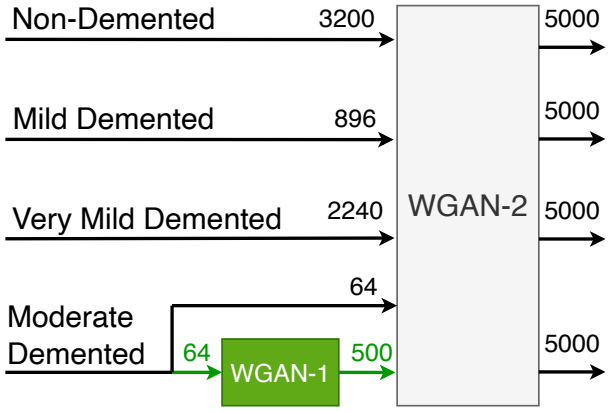


Fig. 3. Block diagram for the proposed Dual-WGAN approach for boosting the Moderate Demented class, and then augmenting the entire dataset.

Despite their impressive capabilities, GANs also have some inherent shortcomings, including but not limited to, Mode Collapse, training convergence issues, and heavy dependence on the data quality and quantity.

Considering that conventional GANs are prone to shortcomings, Wasserstein GAN (WGAN) was developed [19]. A WGAN is essentially a GAN that alters the GAN goal to encourage it to develop interpretable and meaningful representations [20]. The salient features of the WGAN, which are utilized in this work are improved training stability (leading to better convergence) and absence of mode collapse. Because WGAN aids model convergence, we can employ a more complicated model for the generator and discriminator to train it to lean complicated patterns such as those seen in brain MRI images. It is to be noted that in WGANs, the Discriminator is often referred to as a *Critic*.

### C. Methodology and Approach

The methodology adopted in this work is illustrated in Fig. 3. The first WGAN model (WGAN-1) is used for boosting the number of samples in the Moderate Demented class, and is used to generate 500 synthetic images from the 64 real images in that class. Thereafter, the second model, WGAN-2, is employed to augment the entire dataset (all the 4 classes) to generate more synthetic images. It needs to be mentioned that while the proposed Dual-WGAN approach is being illustrated in this work for one chosen dataset for one particular disease, the same approach can readily be employed for the boosting and augmentation of the image dataset for any disease if there is a massive imbalance amongst the different classes.

## IV. Boosting the Moderate Demented Class

This section contains the details of the Generator and Critic models in WGAN-1 used for boosting the minority class.

### A. WGAN-1 Generator Architecture

The architecture and the details of the different layers in the Generator for WGAN-1 model are presented in Table I from where it can be observed that the Generator comprises of 6 `Conv2D` layers interspersed with `UpSampling` and `BatchNormalization` layers. While the first 4 `Conv2D` layers utilize the `ReLU` activation function, the last `Conv2D` layer employs the `tanh` ativation function. The overall parameter count is 1,244,033 out of which 1,242,497 are trainable parameters.

TABLE I
Details of the WGAN-1 Generator Model

| **Generator: Sequential** | | |
|---|---|---|
| **Layer (type)** | **Output Shape** | **Param #** |
| Dense | (None, 2048) | 206848 |
| Reshape | (None, 4, 4, 128) | 0 |
| UpSampling2D | (None, 8, 8, 128) | 0 |
| Conv2D | (None, 8, 8, 256) | 295168 |
| BatchNormalization | (None, 8, 8, 256) | 1024 |
| Activation (ReLU) | (None, 8, 8, 256) | 0 |
| Conv2D | (None, 8, 8, 128) | 295040 |
| BatchNormalization | (None, 8, 8, 128) | 512 |
| Activation (ReLU) | (None, 8, 8, 128) | 0 |
| UpSampling2D | (None, 16, 16, 128) | 0 |
| Conv2D | (None, 16, 16, 128) | 147584 |
| BatchNormalization | (None, 16, 16, 128) | 512 |
| Activation (ReLU) | (None, 16, 16, 128) | 0 |
| UpSampling2D | (None, 32, 32, 128) | 0 |
| Conv2D | (None, 32, 32, 128) | 147584 |
| BatchNormalization | (None, 32, 32, 128) | 512 |
| Activation (ReLU) | (None, 32, 32, 128) | 0 |
| UpSampling2D | (None, 96, 96, 128) | 0 |
| Conv2D | (None, 96, 96, 128) | 147584 |
| BatchNormalization | (None, 96, 96, 128) | 512 |
| Activation (ReLU) | (None, 96, 96, 128) | 0 |
| Conv2D | (None, 96, 96, 1) | 1153 |
| Activation (tanh) | (None, 96, 96, 1) | 0 |
| **Total parameters:** | **1,244,033** | |
| **Trainable parameters:** | **1,242,497** | |
| **Non-trainable parameters:** | **1,536** | |

TABLE II
Details of the Critic Model

| **Critic: Sequential** | | |
|---|---|---|
| **Layer (type)** | **Output Shape** | **Param #** |
| Conv2D | (None, 48, 48, 32) | 320 |
| Activation (LeakyReLU) | (None, 48, 48, 32) | 0 |
| Dropout | (None, 48, 48, 32) | 0 |
| Conv2D | (None, 24, 24, 64) | 18496 |
| ZeroPadding2D | (None, 25, 25, 64) | 0 |
| BatchNormalization | (None, 25, 25, 64) | 256 |
| Activation (LeakyReLU) | (None, 25, 25, 64) | 0 |
| Dropout | (None, 25, 25, 64) | 0 |
| Conv2D | (None, 13, 13, 128) | 73856 |
| BatchNormalization | (None, 13, 13, 128) | 512 |
| Activation (LeakyReLU) | (None, 13, 13, 128) | 0 |
| Dropout | (None, 13, 13, 128) | 0 |
| Conv2D | (None, 13, 13, 128) | 147584 |
| BatchNormalization | (None, 13, 13, 128) | 512 |
| Activation (LeakyReLU) | (None, 13, 13, 128) | 0 |
| Dropout | (None, 13, 13, 128) | 0 |
| Conv2D | (None, 13, 13, 256) | 295168 |
| BatchNormalization | (None, 13, 13, 256) | 1024 |
| Activation (LeakyReLU) | (None, 13, 13, 256) | 0 |
| Dropout | (None, 13, 13, 256) | 0 |
| Flatten | (None, 43264) | 0 |
| Dense | (None, 1) | 43265 |
| **Total parameters:** | **580,993** | |
| **Trainable parameters:** | **579,841** | |
| **Non-trainable parameters:** | **1,552** | |

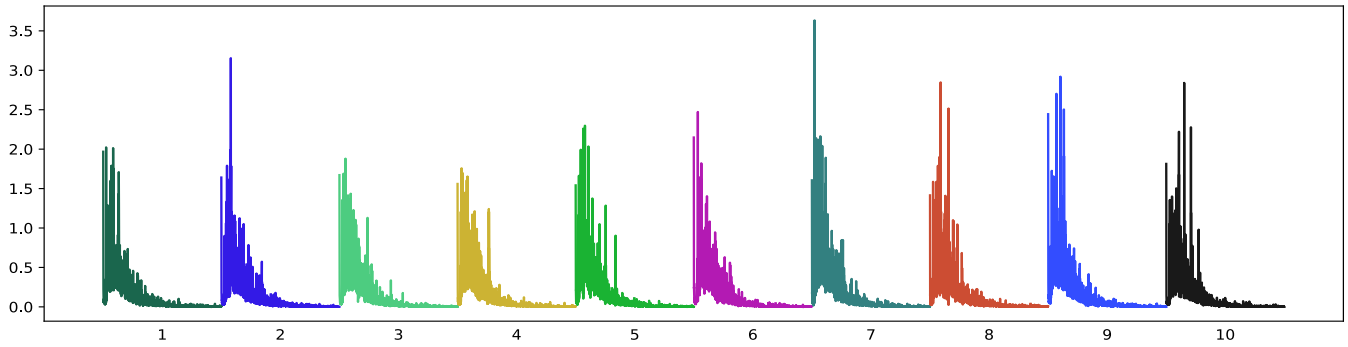


Fig. 4. WGAN-1 Critic Loss plots for the Moderate Demented class for 10 independent trials of 5000 epoch each.

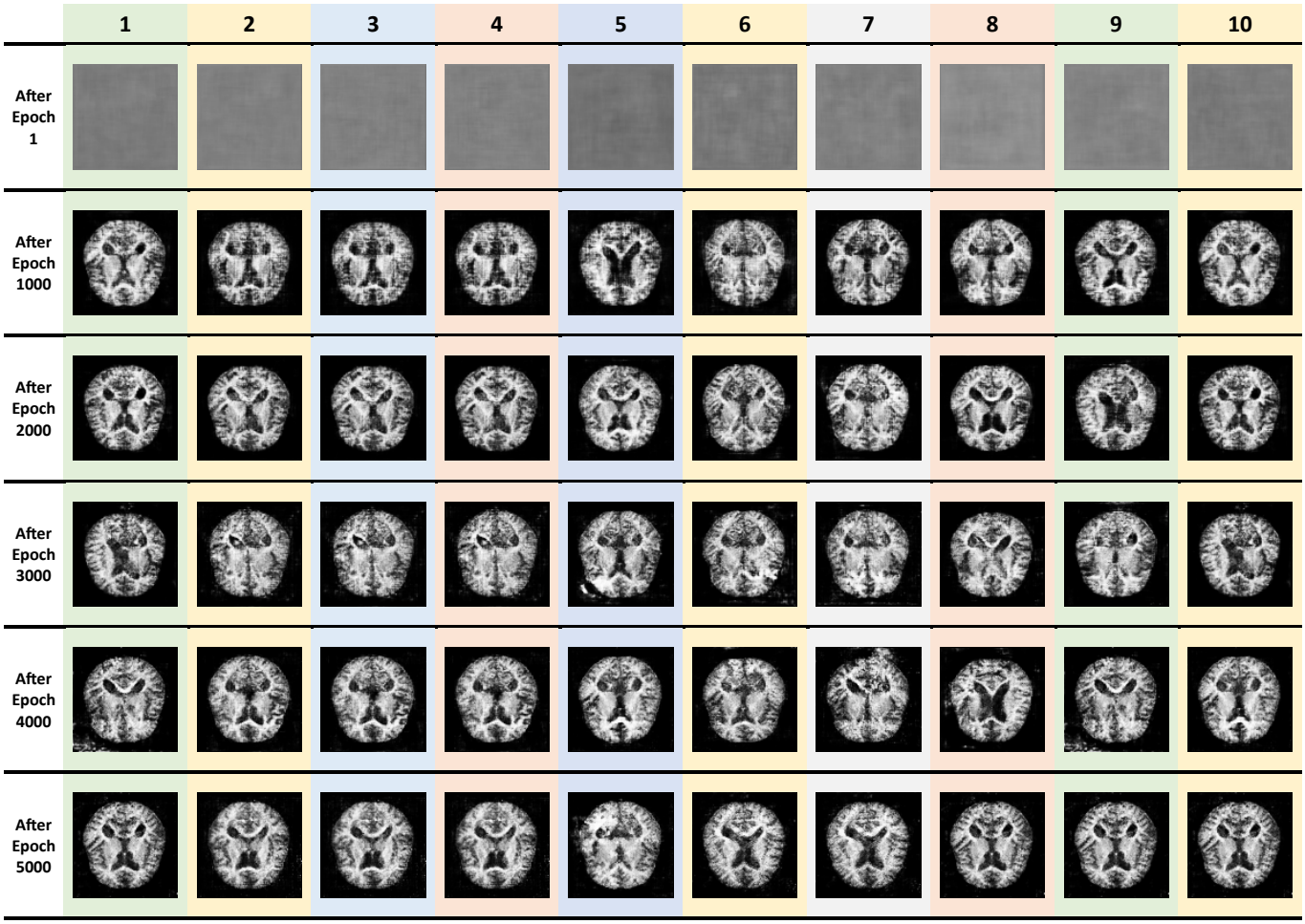


Fig. 5. Generated images for the Moderate Demented class for every 1000 epochs between the first and the last epoch, using WGAN-1.

### *B. WGAN-1 Critic Architecture*

As alluded to earlier, in a WGAN, the Critic is a neural network that assesses the 'quality' of data samples, including both the real samples (i.e. the training data) and the generated samples (produced by the Generator). The architecture and the details of the different layers in the Critic for WGAN-1 model are presented in Table II from where it can be observed that the Critic comprises of 5 `Conv2D` layers interspersed with `Padding` and `BatchNormalization` layers. `Dropout` is also utilized between the successive layers to mitigate overfitting. All the 5 `Conv2D` layers utilize the `LeakyReLU` activation function, while the last `Dense` layer employs the `Sigmoid` activation function. The overall parameter count is 580,993 out of which 579,841 are trainable parameters.

TABLE III
DETAILS OF THE WGAN-2 GENERATOR MODEL

| **Generator: Sequential** | | |
|---|---|---|
| **Layer (type)** | **Output Shape** | **Param #** |
| Dense | (None, 2048) | 206848 |
| Reshape | (None, 4, 4, 128) | 0 |
| UpSampling2D | (None, 8, 8, 128) | 0 |
| Conv2D | (None, 8, 8, 256) | 295168 |
| BatchNormalization | (None, 8, 8, 256) | 1024 |
| Activation (ReLU) | (None, 8, 8, 256) | 0 |
| UpSampling2D | (None, 16, 16, 256) | 0 |
| Conv2D | (None, 16, 16, 256) | 590080 |
| BatchNormalization | (None, 16, 16, 256) | 1024 |
| Activation (ReLU) | (None, 16, 16, 256) | 0 |
| UpSampling2D | (None, 32, 32, 256) | 0 |
| Conv2D | (None, 32, 32, 256) | 590080 |
| BatchNormalization | (None, 32, 32, 256) | 1024 |
| Activation (ReLU) | (None, 32, 32, 256) | 0 |
| UpSampling2D | (None, 96, 96, 256) | 0 |
| Conv2D | (None, 96, 96, 128) | 295040 |
| BatchNormalization | (None, 96, 96, 128) | 512 |
| Activation (ReLU) | (None, 96, 96, 128) | 0 |
| Conv2D | (None, 96, 96, 1) | 1153 |
| Activation (tanh) | (None, 96, 96, 1) | 0 |
| **Total parameters:** | **1,981,953** | |
| **Trainable parameters:** | **1,980,161** | |
| **Non-trainable parameters:** | **1,792** | |

### C. WGAN-1 Results

Next, the results as obtained from the WGAN-1 model are presented. Fig. 4 illustrates the convergence of the proposed WGAN-1 model using its Critic Loss as a metric. The experiment was performed for 10 times, and the differently colored plots in Fig. 4 denote different trials. In WGANs, it is known that the quality of the generated images becomes increasingly better as the Critic Loss keeps decreasing. This indicates that an optimal stopping point for the WGAN training is when the Critic Loss is 'stabilized' i.e. stops decreasing significantly. This is clearly evident in Fig. 4 where the Critic Loss is seen to be reaching a stable minimum state for all the 10 trials.

The output images from the Generator for the different stages of the training process are included in Fig. 5, from where the consistency in the WGAN-1 performance across the 10 trials can be observed.

## V. AUGMENTING THE ENTIRE DATASET

This section presents the details of the WGAN-2 model which is used for the generation of synthetic images for all the 4 classes in the Alzheimer Brian Image dataset.

### A. WGAN-2 Generator and Critic Architectures

The architecture and the details of the different layers in the Critic for WGAN-2 model are presented in Table III from where it can be observed that the Generator for WGAN-2 is less elaborate as compared to the Generator of the WGAN-1 model, and requires lesser number of filters for the different `Conv2D` layers resulting in a significant reduction in the number of trainable parameters. The Critic remains the same as the one utilized for WGAN-1.

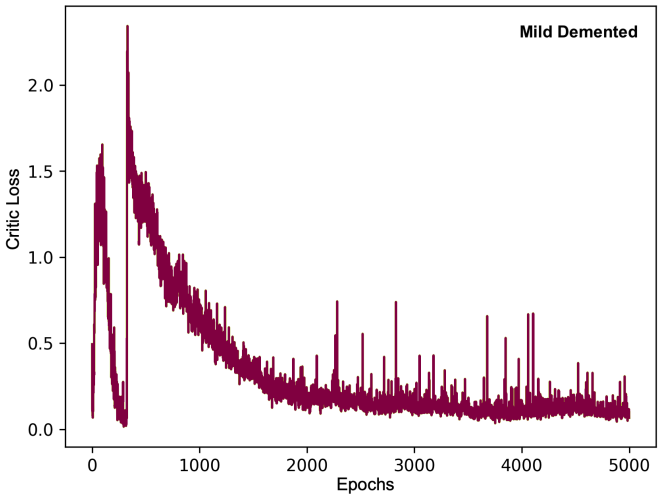


Fig. 6. WGAN-2 Critic Loss plot for the Mild Demented class

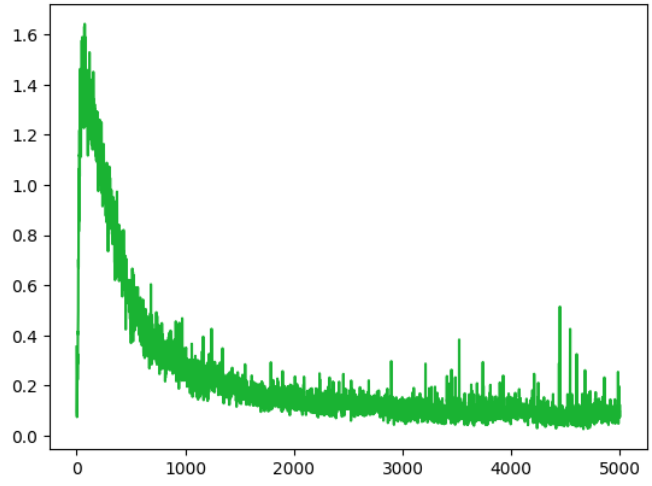


Fig. 7. WGAN-2 Critic Loss plot for the Very Mild Demented class

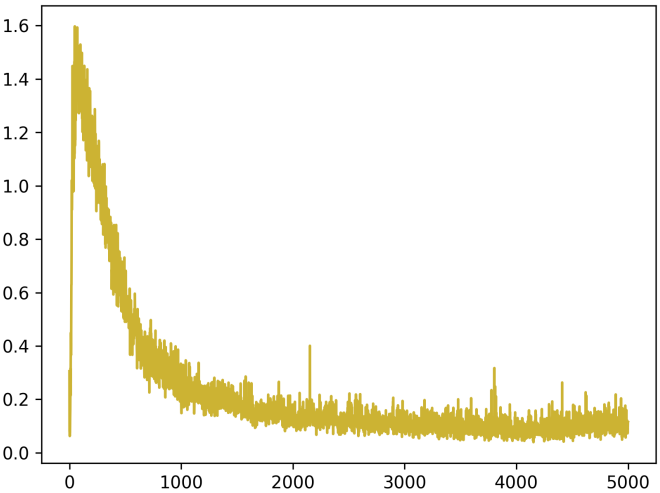


Fig. 8. WGAN-2 Critic Loss plot for the Non-Demented (Normal) class

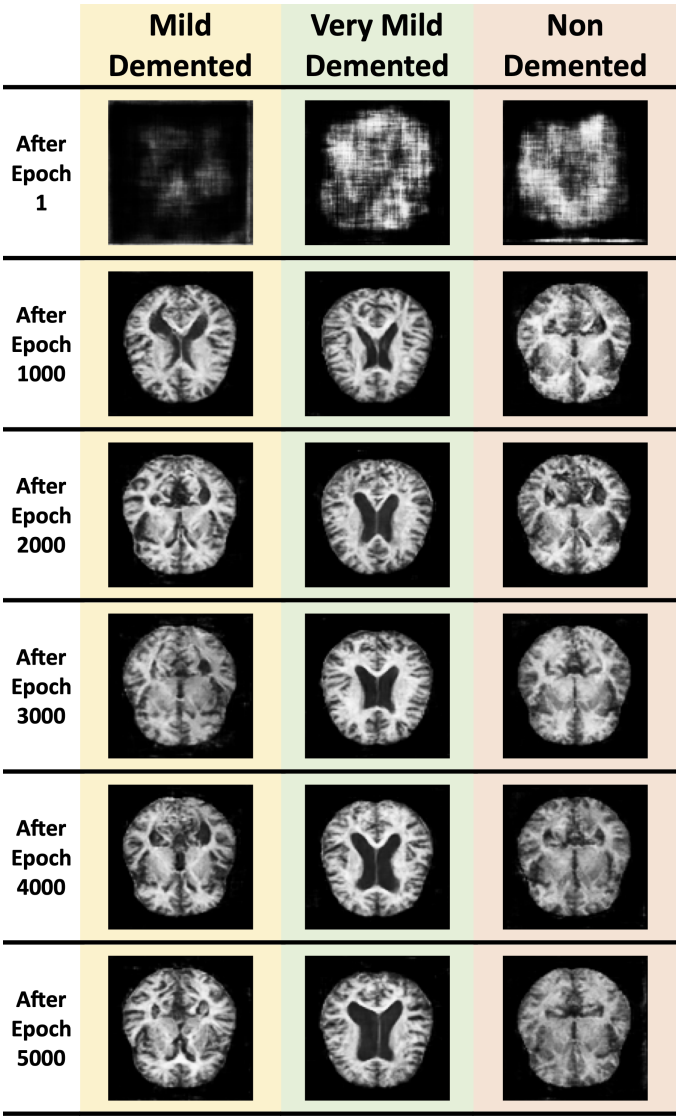


Fig. 9. WGAN-2 generated imagesd for Mild Demented, Very Mild Demented, and Non Demented (Normal) classes, for every 1000 epcohs between 0 and 5000 epochs

### *B. WGAN-2 Results*

This section presents the results of the dataset augmentation as performed using WGAN-2. For the 'Mild Demented' class, the Critic Loss plot and samples of generated images are presented in Fig. 6 and Fig. 9(first column) respectively. From Fig. 6 it can be observed that the Critic Loss does indeed stabilizes after around 3000 epochs.

Another pertinent observation from Fig. 6 is that the image generated after the first epoch in this case is 'better' than the one generated for the Moderate Demented case (in Fig. 6). This could be attributed to the Generator learning better due to the higher number of training samples (896 versus 64). However, the spikes in the Critic Loss plot even after the training for 2000 epochs indicate that due to the varying nature of the samples in the Mild Demented dataset, the quality of the generated images stabilizes well after the 4000 epoch point, where the training may be stopped.

Similarly, for the Very Mild Demented class, the Critic Loss plot is presented in Fig. 7 from where it can be observed that the optimal Loss values appear just before the 3000 epoch point. This can also be observed from Fig. 9 where for the Very Mild Demented outputs, the quality of the generated images diminishes after the 4000 epoch mark. Lastly, although not required for this dataset (since this dataset already has the Normal class as the majority class), for the sake of completion, the Non-Demented class of images was also generated using the WGAN-2, and the Critic Loss plot and the generated images are presented in Fig. 8 and Fig. 9 respectively.

## VI. Conclusion

In this paper, we introduced a Dual-WGAN-based boosting and augmentation technique for first generating synthetic images for the minority class, and then augmenting the entire 4-class Alzheimer dataset. This is relevant to the current research landscape, where advanced deep learning models exist for disease detection but are constrained by the availability of high-quality and sufficient training data. The approach presented in this paper offers a solution by augmenting existing datasets with high-quality synthetic images.

## References

[1] T. Jo, K. Nho, and A. J. Saykin, "Deep learning in alzheimer's disease: diagnostic classification and prognostic prediction using neuroimaging data," *Frontiers in aging neuroscience*, vol. 11, p. 220, 2019.

[2] British Broadcasting Corporation (BBC), "New alzheimer's drug slows disease by a third," https://www.bbc.co.uk/news/health-65471914, Last Accessed: 2023-05-3.

[3] World Health Organization (WHO), "Dementia," https://www.who.int/news-room/fact-sheets/detail/dementia, Last Accessed: 2023-03-24.

[4] J. E. Galvin, "Prevention of alzheimer's disease: Lessons learned and applied," *Journal of the American Geriatrics Society*, 2017.

[5] M. W. Schelke, P. Attia, D. J. Palenchar, B. Kaplan, M. Mureb, C. A. Ganzer, O. Scheyer, A. Rahman, R. Kachko, R. Krikorian *et al.*, "Mechanisms of risk reduction in the clinical practice of alzheimer's disease prevention," *Frontiers in aging neuroscience*, vol. 10, p. 96, 2018.

[6] D. P. Veitch, M. W. Weiner, P. S. Aisen, L. A. Beckett, N. J. Cairns, R. C. Green, D. Harvey, C. R. Jack Jr, W. Jagust, J. C. Morris *et al.*, "Understanding disease progression and improving alzheimer's disease clinical trials: Recent highlights from the alzheimer's disease neuroimaging initiative," *Alzheimer's & Dementia*, vol. 15, no. 1, pp. 106–152, 2019.

[7] S. S. A. Zaidi, M. S. Ansari, A. Aslam, N. Kanwal, M. Asghar, and B. Lee, "A survey of modern deep learning based object detection models," *Digital Signal Processing*, p. 103514, 2022.

[8] M. Khojaste-Sarakhsi, S. S. Haghighi, S. F. Ghomi, and E. Marchiori, "Deep learning for alzheimer's disease diagnosis: A survey," *Artificial Intelligence in Medicine*, p. 102332, 2022.

[9] S. Sarraf and G. Tofighi, "Classification of alzheimer's disease using fmri data and deep learning convolutional neural networks," 2016. [Online]. Available: https://arxiv.org/abs/1603.08631

[10] P. Isola, J.-Y. Zhu, T. Zhou, and A. A. Efros, "Image-to-image translation with conditional adversarial networks," 2016. [Online]. Available: https://arxiv.org/abs/1611.07004

[11] J. Ho and S. Ermon, "Generative adversarial imitation learning," in *Advances in Neural Information Processing Systems*, D. Lee, M. Sugiyama, U. Luxburg, I. Guyon, and R. Garnett, Eds., vol. 29. Curran Associates, Inc., 2016.

[12] J. Park, H. Kim, J. Kim, and M. Cheon, "A practical application of generative adversarial networks for rna-seq analysis to predict the molecular progress of alzheimer's disease," *PLOS Computational Biology*, vol. 16, p. e1008099, 07 2020.

[13] T. Bai, M. Du, L. Zhang, L. Ren, L. Ruan, Y. Yang, G. Qian, Z. Meng, L. Zhao, and M. J. Deen, "A novel alzheimer's disease detection approach using gan-based brain slice image enhancement," *Neurocomputing*, vol. 492, pp. 353–369, 2022.

[14] C. Han, L. Rundo, K. Murao, Z. Milacski, K. Umemoto, E. Sala, H. Nakayama, and S. Satoh, "Gan-based multiple adjacent brain mri slice reconstruction for unsupervised alzheimer's disease diagnosis," 2019. [Online]. Available: https://arxiv.org/abs/1906.06114

[15] X. Zhou, S. Qiu, P. S. Joshi, C. Xue, R. J. Killiany, A. Z. Mian, S. P. Chin, R. Au, and V. B. Kolachalama, "Enhancing magnetic resonance imaging-driven alzheimer's disease classification performance using generative adversarial learning," *Alzheimer's research & therapy*, vol. 13, no. 1, pp. 1–11, 2021.

[16] J. Islam and Y. Zhang, "Gan-based synthetic brain pet image generation," *Brain Informatics*, vol. 7, 03 2020.

[17] I. Garali, M. Adel, S. Bourennane, and E. Guedj, "Classification of positron emission tomography brain images using first and second derivative features," in *2016 6th European Workshop on Visual Information Processing (EUVIP)*, 2016, pp. 1–5.

[18] Y. LeCun, Y. Bengio, and G. Hinton, "Deep learning," *Nature*, vol. 521, pp. 436–44, 05 2015.

[19] M. Arjovsky, S. Chintala, and L. Bottou, "Wasserstein generative adversarial networks," in *Proceedings of the 34th International Conference on Machine Learning*, ser. Proceedings of Machine Learning Research, D. Precup and Y. W. Teh, Eds., vol. 70. PMLR, 06–11 Aug 2017, pp. 214–223. [Online]. Available: https://proceedings.mlr.press/v70/arjovsky17a.html

[20] B. Z. Hussain, I. Andleeb, M. S. Ansari, A. M. Joshi, and N. Kanwal, "Wasserstein gan based chest x-ray dataset augmentation for deep learning models: Covid-19 detection use-case," in *2022 44th Annual International Conference of the IEEE Engineering in Medicine & Biology Society (EMBC)*. IEEE, 2022, pp. 2058–2061.